Weislander, L. (1979) *Anal. Biochem. 98*, 305–309.
Williams, A. F. (1987) *Immunol. Today 8*, 298–303.
Williams, A. F., & Barclay, A. N. (1988) *Annu. Rev. Immunol. 6*, 381–405.
Yoshitake, S., Schach, B. G., Foster, D. C., Davie, E. W., & Kurachi, K. (1985) *Biochemistry 24*, 3736–3750.
Zimmermann, W., Ortlieb, B., Friedrich, R., & von Kleist, S. (1987) *Proc. Natl. Acad. Sci. U.S.A. 84*, 2960–2964.

An NMR Study of the Covalent and Noncovalent Interactions of CC-1065 and DNA

Terrence A. Scahill,* Randy M. Jensen, David H. Swenson,‡ Nicole T. Hatzenbuhler, Gary Petzold, Wendell Wierenga, and Nanda D. Brahme§

Research Laboratories, Pharmaceutical Research and Development Division, The Upjohn Company, Kalamazoo, Michigan 49001

Received August 8, 1989; Revised Manuscript Received November 16, 1989

ABSTRACT: The binding of the antitumor drug CC-1065 has been studied with nuclear magnetic resonance (NMR) spectroscopy. This study involves two parts, the elucidation of the covalent binding site of the drug to DNA and a detailed investigation of the noncovalent interactions of CC-1065 with a DNA fragment through analysis of 2D NOE (NOESY) experiments. A CC-1065–DNA adduct was prepared, and an adenine adduct was released upon heating. NMR (^{1}H and ^{13}C) analysis of the adduct shows that the drug binds to N3 of adenine by reaction of its cyclopropyl group. The reaction pathway and product formed were determined by analysis of the ^{13}C DEPT spectra. An octamer duplex, d(CGATTAGC·GCTAATCG), was synthesized and used in the interaction study of CC-1065 and the oligomer. The duplex and the drug–octamer complex were both analyzed by 2D spectroscopy (COSY,NOESY). The relative intensity of the NOEs observed between the drug (CC-1065) and the octamer duplex shows conclusively that the drug is located in the minor groove, covalently attached to N3 of adenine 6 and positioned from the 3′ → 5′ end in relation to strand A [d(CGATTA^{6}GC)]. A mechanism for drug binding and stabilization can be inferred from the NOE data and model-building studies.

CC-1065, a fermentation product of *Streptomyces zelensius*, was one of the most cytotoxic antitumor agents known when discovered (Hanka et al., 1978):

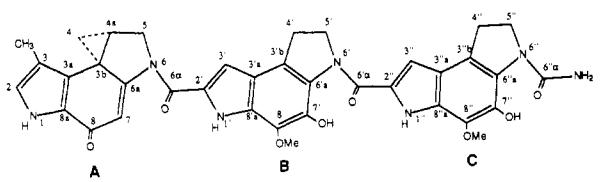

The isolation and characterization of this antibiotic has been reported (Martin et al., 1980, 1981), and the X-ray crystal study including an interaction study of CC-1065 with DNA was published shortly thereafter (Chidester et al., 1981). The antibiotic has a unique structure possessing a cyclopropyl ring with alkylating potential and a twist or pitch in the backbone of the molecule giving it a half-moon or banana shape with concave and convex sides. This structural feature permits a compatible fit in the minor groove of DNA. Experimental evidence for minor groove binding includes competitive binding studies with netropsin, site-exclusion studies, and reduction of the alkylation of minor groove sites after treatment of the DNA with methylation agents (Swenson et al., 1982). Molecular model building using CPK models and computer graphics have also been used to understand the drug–DNA interaction in a qualitative way.

(+)-CC-1065 was shown to be efficacious in the treatment of experimental tumors in mice (Reynolds et al., 1986; Martin et al., 1981). Unfortunately, (+)-CC-1065 also produced delayed death in mice at therapeutic doses (McGovern et al., 1984), and subsequently, its development was halted. However, this lead compound has led to the development of potent, efficacious analogues that do not cause delayed death and are promising as therapeutic agents (Warpehoski et al., 1986; Li et al., 1987).

Preliminary reports (Hurley et al., 1984; Scahill et al., 1986) detailed the structure of the adduct formed upon reaction with calf thymus (CT)[1] DNA, and two others demonstrating the sequence specificity of the drug with DNA have also appeared (Reynolds et al., 1986; Hurley et al., 1988). While CC-1065 interacts with DNA and is thought to exhibit its cytotoxic effects through disruption of DNA synthesis, the exact nature of the DNA binding has been elusive. Circular dichroism (CD) studies (Krueger et al., 1985, 1987) suggest strong binding to duplex DNA, especially sequences rich in adenine–thymine (A-T) base pairs. CC-1065 and DNA interact

* Author to whom correspondence should be addressed.
‡ Present address: Visiting Scientist at the National Center for Toxicological Research, Jefferson, AR 72079.
§ Present address: Bio-Rad Laboratories, 1000 Alfred Nobel Dr., Hercules, CA 94547.

[1] Abbreviations: NMR, nuclear magnetic resonance; NOE, nuclear Overhauser effect; COSY, homonuclear correlated spectroscopy; NOESY, two-dimensional NOE correlated spectroscopy; COLOC, correlated spectroscopy with long-range coupling; DEPT, distortionless enhancement with polarization transfer; CT, calf thymus; FID, free induction decay; CD, circular dichroism; HPLC, high-performance liquid chromatography.

0006-2960/90/0429-2852$02.50/0

by two separate modes of mechanisms as evidenced by the change in CD ellipticity curves during a 72-h period. The first mode is reversible and noncovalent in nature and is little understood. It is thought that this interaction is preliminary to and part of the drug's search for specific nucleotide sequences. The second mode of binding is irreversible and has been shown to be covalent in nature. Thus, elucidation of the binding of the parent drug to a DNA fragment that includes the target sequence is very important. This knowledge is necessary not only to obtain a fundamental understanding of how CC-1065 and analogues work on the molecular level but also to aid in the rational design of potent and useful drugs based on the parent drug.

This paper is concerned with two main themes, the first being the formation, isolation, and characterization of the adduct formed when CC-1065 and DNA react, i.e., the covalent interaction. NMR analysis including 2D ^1H–^1H correlated spectroscopy (COSY) at 500 MHz and ^{13}C polarization transfer experiments (DEPT) show that a covalent bond is indeed formed between the antitumor agent and CT DNA. The NMR analysis determined the precise location of the covalent bond and the structure of the DNA adduct.

The second theme concerns the interactions (covalent and noncovalent) between CC-1065 and a DNA fragment. The DNA fragment was synthesized to specifically explore these interactions and to begin study of the sequence specificity of this drug. An unsymmetrical octamer duplex (5′-CGATTAGC-3′) and its complement were prepared and used for the drug–DNA studies. A multitude of 2D NMR experiments were performed to assign the ^1H spectra of the octamer duplex and the CC-1065 complex. Analysis of the 1D and 2D NOE experiments provides insight into the localization of the drug with respect to the DNA sequence. Thus NMR has been used to examine the covalent binding site, the direction of the drug with respect to the duplex, and noncovalent interactions between the drug and the duplex in the minor groove.

Experimental Procedures

Synthesis of the CC-1065–DNA Adduct. CC-1065 [52 mg, 72 μmol, in 26 mL of dimethylformamide (DMF)] was reacted with calf thymus DNA (1 g) in 500 mL of 10 mM sodium phosphate buffer, pH 7.4. After precipitation with sodium chloride and ethanol, the material was dissolved in 500 mL of 10 mM sodium phosphate buffer, pH 7.4, and heated at 100 °C with 500 mL of 1-butanol. The sample was frequently shaken to emulsify. At 25 min the phases were separated, and the aqueous component was further heated with 400 mL of 1-butanol for 25 min. The butanol extracts were combined and analyzed for the CC-1065 chromophore. The combined butanol extracts were brought to dryness at 40 °C in vacuo, and the residue was dissolved in 7.7 mL of 70% DMF. After the residue had been washed into the column with 4 mL of 70% DMF, the column was eluted at about 0.45 mL/min with 70% DMF. Fractions (9 mL) were examined by chromatography on Whatman CS5 Multi-K reversed-phase thin-layer plates in 70% DMF. The large-scale preparation of the adduct isolated by extraction with hot butanol yielded 60 μmol (~50 mg) of adduct on the basis of the assumption that its molar extinction coefficient is the same as that of CC-1065 (48 000 at 365 nm). Aliquots of fractions examined by thin-layer chromatography on the Multi-K reversed-phase plates developed with 70% DMF showed a single component with an R_f of 0.55. This material (~28 μmol) was brought to dryness in vacuo, dissolved in deuterated DMF-d_7, redried, redissolved in deuterated DMF, and filtered through glass wool into an NMR tube.

Synthesis of the DNA Octamer Duplex and Sample Preparation. The octanucleotide 5′-d(CGATTAGC)-3′ and its complement were synthesized according to the solid-phase phosphoramidite triester coupling approach (Beaucage & Caruthers, 1982) on a BioSearch SAMI DNA synthesizer as described earlier (Needham-Vandevanter et al., 1984). Both oligomers were purified by anion-exchange HPLC using a PEI-coated silica column functionalized according to a procedure already described (Pearson & Regnier, 1983). By use of a stepwise gradient of triethylammonium bicarbonate, separation of product from failure sequences was obtained. The triethylammonium salt of the oligomers was converted to sodium by running the purified 8-mer through a Na^+ resin column. Water was used as the elution buffer. The oligonucleotide solutions were then lyophilized. Fifty-six OD units of each oligonucleotide was annealed in 0.5 mL of 10 mM Na_3PO–100 mM NaCl (pH 7.0) by incubation at 65 °C for 30 min followed by a slow cool down to room temperature over a 4.5-h period. Approximately 1 mg of the CC-1065–CT DNA adduct dissolved in DMF-d_7 was used for both the proton (1D and 2D) and carbon (DEPT) experiments. NMR samples of the octamer duplex were prepared by dissolving approximately 4 mg of the duplex in 0.45 mL of a buffer containing 10 mM sodium phosphate and 100 mM NaCl (pH 7.1). For experiments with only nonexchangeable protons this solution was lyophilized (twice) to dryness and redissolved in 99.996% D_2O. A small amount of TSP [sodium 3-(trimethylsilyl)propionate-*2,2,3,3-d*$_4$] was added as an internal reference. The drug–duplex adduct was prepared by adding an excess amount of CC-1065 (49 μL of a 6 mg of CC-1065/mL of DMF-d_7 solution) to the duplex solution. After being allowed to stand overnight the excess CC-1065 was removed by filtration, and the sample was lyophilized and redissolved in 99.996% D_2O.

NMR Spectroscopy. All NMR spectra were obtained on a Bruker AM-500 spectrometer equipped with an Aspect-3000 computer, an array processor, and digital phase shifting hardware. Proton–proton correlated (COSY) experiments (both absolute value mode and double-quantum filtered phase sensitive) were acquired with the standard pulse sequence (Aue et al., 1976; Bax & Freeman, 1981). A total of 512 experiments (256 scans each) were collected by use of 2048 complex points in t_2 with incrementation of t_1 from 2 μs to 1 ms. The phase-sensitive COSY experiment was performed according to the time proportional phase incrementation (TPPI) method (Redfield & Kuntz, 1975; Bodenhausen et al., 1980) as described by Marion and Wuthrich (1983). The time domain spectra were multiplied in both dimensions by a sine-bell window function (shifted $\pi/8$ in t_2 and $\pi/4$ in t_1) and zero-filled to 1024 points in the t_1 dimension. Fourier transformation gave a 2D data matrix of 1K × 1K real points with 4.8 Hz/point digital resolution in each dimension. NOE correlated (NOESY) spectra (Kumar et al., 1980; Macura et al., 1981; Wider et al., 1984) were also obtained in the phase-sensitive mode (TPPI). A total of 650 experiments (160 scans each) were collected with 2K complex points. The time domain spectra were multiplied by a line-broadening function (6 Hz) in the t_2 domain and a Gaussian filter (or cosine window) in t_1. NOE difference spectra were obtained by interleaving the decoupler pulse on and off resonance every 16 scans with quadrature phase cycling. In a typical experiment the entire cycle was repeated 50–100 times. A saturation pulse with a duration of 0.5–2.0 s was used, and the decoupler power was adjusted to just saturate the irradiated peak and yet minimize any effects on any neighboring ab-

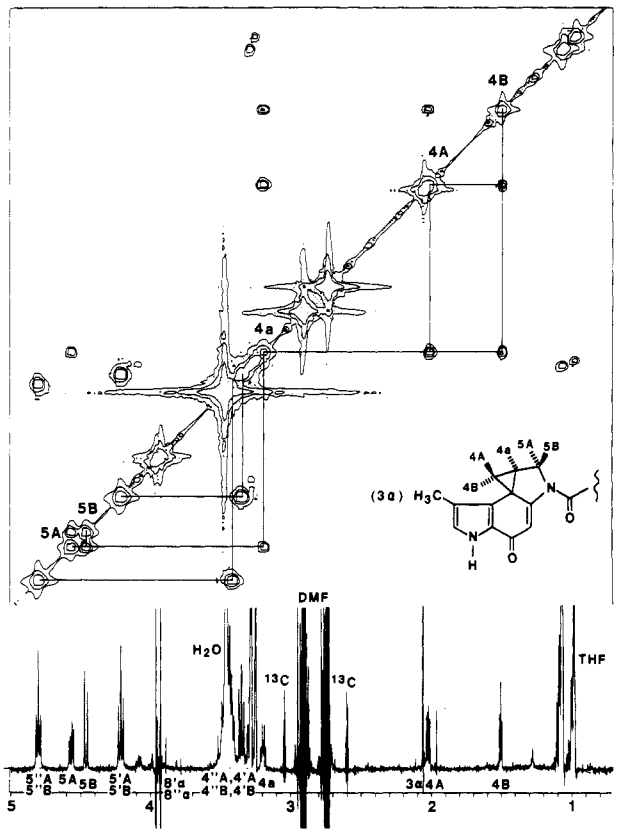

FIGURE 1: 2D COSY contour plot of the upfield region (1–5 ppm) of CC-1065 (1 mM) in DMF-d_7. A 1D spectral trace is presented for convenient reference at the bottom of the contour plot. All aliphatic protons are labeled, and the A ring spin system is shown with its connectivities traced out on the contour plot.

sorptions. The free induction decays (FIDS) were processed with an identical window function (LB = 3 Hz) and the same zero- and first-order phase constants. Finally, spectra were subtracted. For measurement in H_2O, spectra were acquired by a semiselective "jump and return" sequence (90_x–t–90_{-x}) (Plateau & Gueron, 1982). All NMR spectra were obtained at 25 °C.

Results and Discussion

Characterization of CC-1065. Preliminary ^1H and ^{13}C NMR data on CC-1065 have been published (Hurley et al., 1984); however, extensive work using 2D heterocorrelated techniques has not been completed. These new data confirm many assignments but also require some assignment changes, especially the ^{13}C assignments of the quaternary aromatic carbons. The ^1H and ^{13}C chemical shifts for the drug are shown in Tables I and II, respectively. A battery of 2D techniques including COSY, (^1H–^{13}C) heterocorrelated, and COLOC experiments were used to determine all the proton and carbon line assignments. Figure 1 shows a contour plot of a representative COSY experiment detailing the correlations of the protons in the cyclopropyl ring system in the parent molecule (CC-1065). Figure 2 shows a contour plot of a 2D (^1H–^{13}C) heterocorrelated experiment of CC-1065 which relates all the proton and carbon chemical shifts. The positions of the quaternary carbons were established by several COLOC experiments with slightly different delay times to enhance specific long-range couplings. The assignments of the carbon chemical shifts are based on the analysis of the above 2D experiments in addition to correlations with model compounds (analogues) and multiplicity data derived from DEPT experiments.

Table I: ^1H Chemical Shifts[a] of CC-1065 Compounds

assignment	CC-1065	CC-1065–adenine adduct
2	6.97	7.19
3′	7.19	6.97
3″	7.19	6.90
3α	2.06	2.65
4A	2.03 [J(4A,4B) = 7.6]	4.68 [J(4A,4B) = 11.3]
4B	1.50 [J(4B,4a) = 4.1]	4.42 [J(4B,4a) = 0]
4a	3.20 [J(4A,4a) = 4.5]	4.63 [J(4A,4a) = 7.3]
5A	4.57	4.85
5B	4.46	4.42
4′A	3.35	3.35
4′B	3.35	3.35
5′A	4.21	4.22
5′B	4.21	4.22
4″A	3.42	3.35
4″B	3.42	3.35
5″A	4.81	4.77
5″B	4.81	4.77
7	6.63	6.97
8′α(OCH_3)	3.93	3.93
8″α(OCH_3)	3.96	3.99
Ade-H2		7.80
Ade-H8		8.06

[a] All chemical shifts are in ppm relative to TSP.

Table II: ^{13}C Chemical Shifts[a] of the CC-1065 Series

assignment	CC-1065	CC-1065-OAc	CC-1065–adenine adduct
3α-CH_3	9.89	11.10	11.96
4	21.74	66.70	54.76
4a	21.86	39.80	40.14
4″	27.47	27.10	27.46
4′	28.48	28.10	28.49
3b	32.42	110.40	109.80
5″	50.34	50.00	50.34
5′	54.21	53.80	54.17
5	55.70	55.20	54.39
8′	60.38	60.10	60.39
8″	60.68	60.40	60.69
3′	106.67	104.40	104.34
3″	107.02	106.60	106.87
7	111.75	98.00	98.40
3	114.09	112.10	112.70
2′	118.40	118.10	118.40
2″	118.90	118.70	119.00
3b″	119.10	119.10	119.10
3b′	122.10	121.70	121.70
2	124.02	124.60	124.94
3a	128.00	125.40	125.60
6a′	128.60	128.10	128.10
6a″	128.60	128.70	128.60
3a″	130.10	130.30	130.21
8a	130.20	125.40	125.87
3a′	130.70	130.30	130.63
8a″	131.44	130.80	131.00
8a′	131.98	132.80	133.20
7′	133.44	133.50	133.46
7″	134.12	134.20	134.11
8′	139.43	130.70	138.92
8″	139.79	139.00	139.37
6α″	158.68	158.40	158.70
6α	161.15	137.20	137.72
6α′	161.72	161.30	161.59
6	162.00	160.40	160.32
8	177.45	144.20	144.55

[a] All chemical shifts are in ppm relative to TSP.

Characterization of the CC-1065–Adenine Adduct. The derivation of the CC-1065–adenine adduct along with preliminary NMR analysis has been previously disclosed (Hurley et al., 1984). In this paper the (+)-CC-1065–adenine adduct was characterized by 1D and 2D ^1H and ^{13}C experiments. Tables I and II list the ^1H and ^{13}C chemical shifts for the

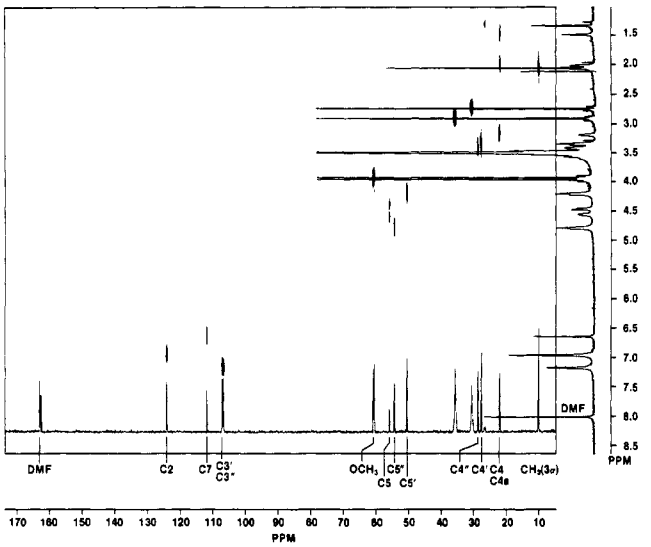

FIGURE 2: 2D contour plot of the 2D heterocorrelated (^{1}H–^{13}C) experiment of CC-1065 in DMF-d_7. A ^{13}C projection is plotted along the ^{13}C axis (F_2 axis) and a 1D ^{1}H spectrum of CC-1065 is plotted along the F_1 axis for reference.

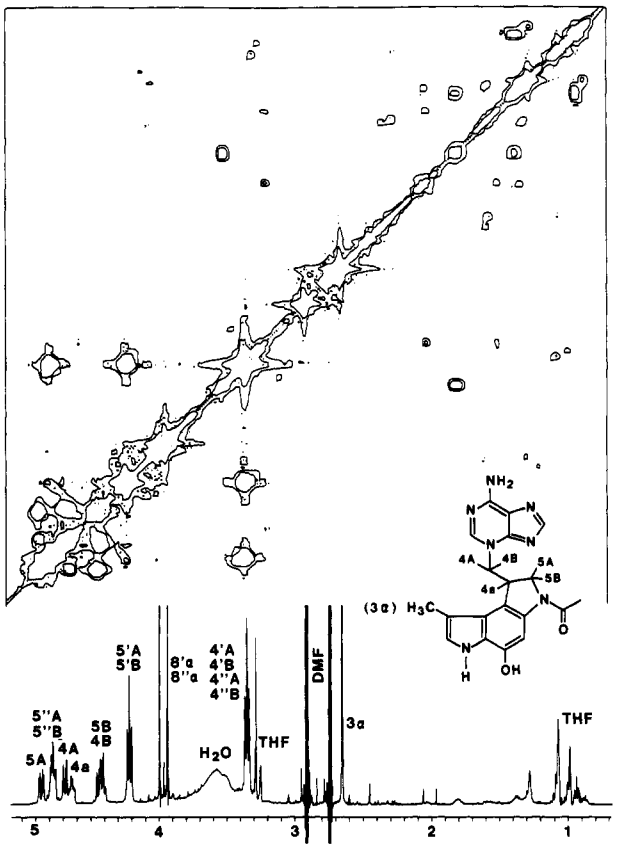

FIGURE 3: 2D COSY contour plot of the upfield region (1–5 ppm) of the CC-1065–adenine adduct after cleavage from calf thymus DNA. The A ring portion of CC-1065 is shown, and all aliphatic assignments are presented on the plot.

adduct. Figure 3 shows an expanded region of a contour plot from a COSY experiment on the adduct. It is immediately apparent from the data that the cyclopropyl ring system has opened since the cyclopropyl hydrogens have shifted downfield into the region occupied by the methylene hydrogens of the B and C rings (compare Figure 3 to Figure 1). The B and C ring systems are difficult to analyze because the chemical shifts of the methylenes of the dihydropyrrole in the B and C rings are nearly identical and the patterns are complex. However, at 500 MHz all the correlations can be discerned,

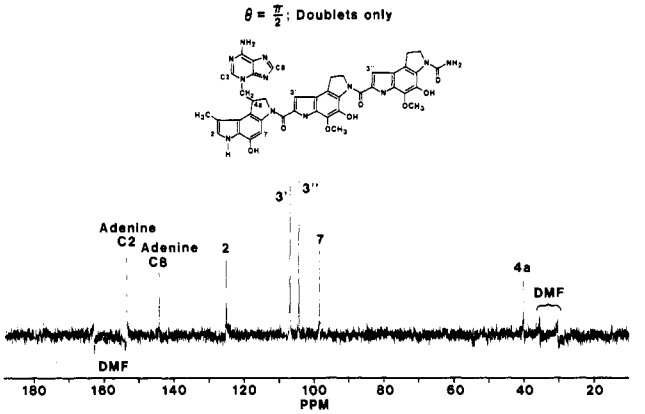

FIGURE 4: DEPT spectrum of the CC-1065–adenine adduct. This spectrum optimized for CH's (doublets) was obtained with the θ pulse of $\pi/2$.

Scheme I

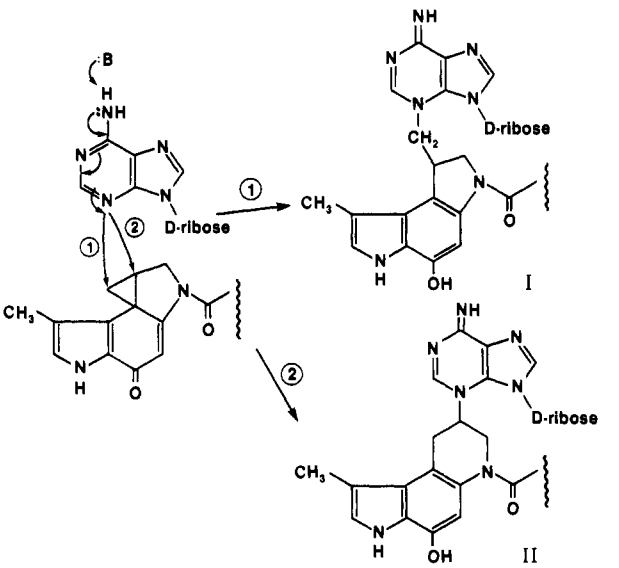

and each hydrogen is assigned in the CC-1065–adenine adduct. Some representative assignments and their correlations are shown on the COSY contour plot in Figure 3.

Two possible reaction pathways can occur when the N3 of adenine reacts with the cyclopropyl group of CC-1065. These pathways are depicted in Scheme I, where partial CC-1065 structures are shown. Two reaction products are possible (structures I and II), and the proton spectrum of the CC-1065–adenine adduct is reasonable for both of these products. The correct structure of the adduct was determined by analysis of ^{13}C NMR data. Figure 4 shows a DEPT spectrum of the adduct where only doublets (CH carbons) are selected. This is accomplished by setting the appropriate time delays in the DEPT procedure. The crucial ^{13}C NMR line is the doublet that appears at 40.1 ppm, and this resonance can only be assigned to the methine that results from the opening of the cyclopropyl ring (i.e., 4a in the structure of CC-1065). The chemical shift of this methine carbon (C4a; 40.1 ppm) shows that the adduct is structure I as shown Scheme I. This is a reasonable chemical shift for a methine carbon adjacent to two methylene carbons (C4, C5) and an aromatic system (A ring). On the other hand, if the methine (C4a) were adjacent to adenine N3 as in structure II, it would be shifted to a much lower field (>50 ppm). Note that the *methylene* carbon (C4) that is adjacent to N3 of adenine in structure I appears at 54.76 ppm. These arguments are supported by the shifts of model compounds; for example, C4a in CC-1065-OAc (Martin

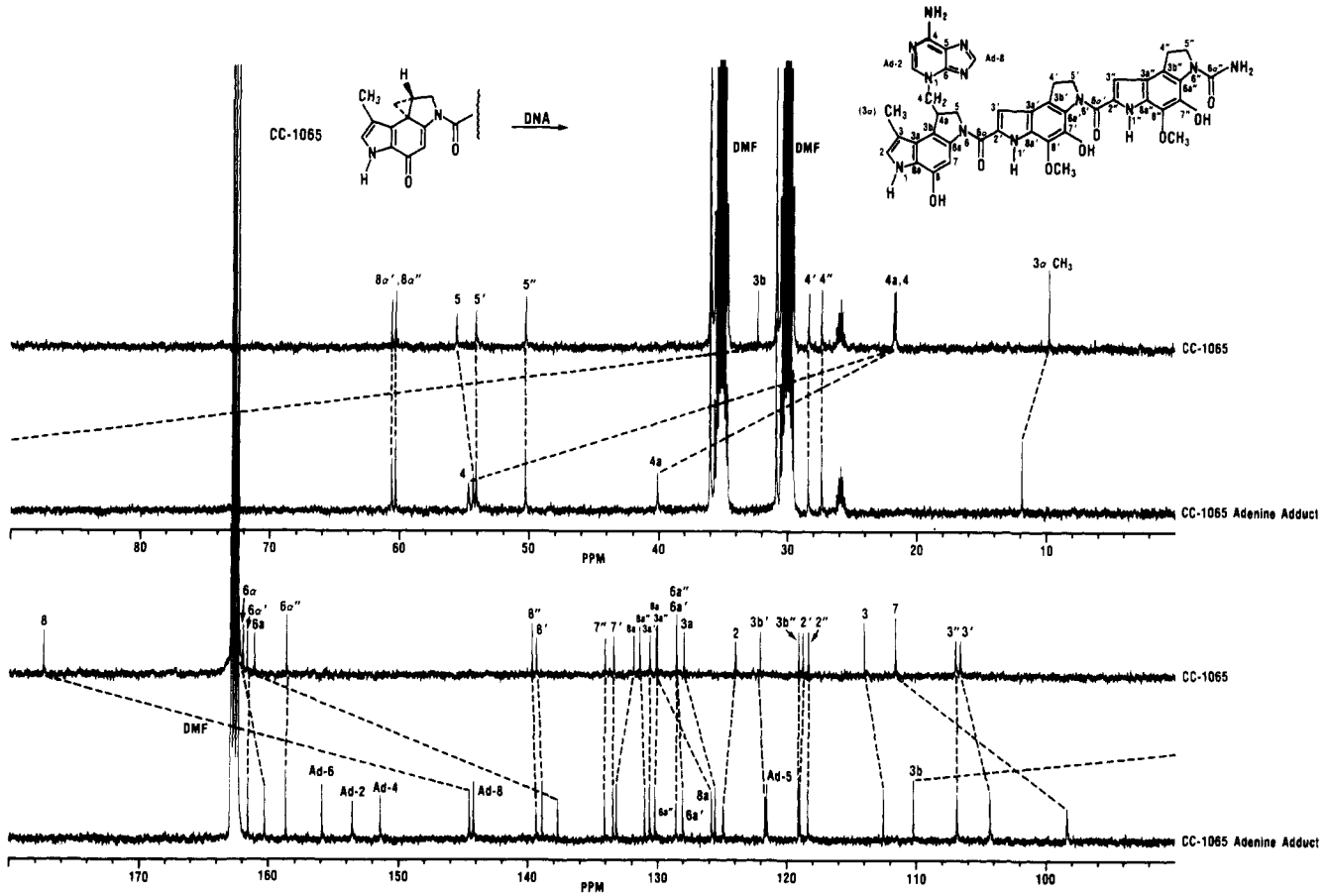

FIGURE 5: Comparison of the ^{13}C spectra of CC-1065 and the CC-1065–adenine adduct. The dashed lines trace the chemical shift changes of the various carbons. Note the large chemical shift changes of the A ring carbons and cyclopropyl carbons.

Table III: ^{13}C Chemical Shift[a] Comparison

carbon	CC-1065–adenine adduct	3-methyladenine
C2	153.7	153.6
C4	151.5	150.6
C5	121.5	120.3
C6	155.9	155.6
C8	144.4	146.2

[a] Chemical shifts are in ppm relative to TMS.

et al., 1985) (Table II) appears at 39.8 ppm, and the aromatic shifts of 3-methyladenine (Table III) agree with that observed in the CC-1065–adenine adduct. The other carbon line assignments for the adduct were determined by 2D heterocorrelated experiments including several COLOC experiments. A comparison of the carbon spectra of the drug and adenine adduct is shown in Figure 5, where the connecting lines depict the changes in chemical shift of pertinent carbons and identification of the carbon lines of the adenine moiety. The spectra show that the largest changes are at the cyclopropyl carbons: C4 (+23.02 ppm), C4a (+18.28 ppm), C3b (+77.38 ppm), and the A ring system carbons C6a (−23.43 ppm), C7 (−13.25 ppm), C8 (−32.9 ppm), C8a (−4.33 ppm), and C3a (−2.4 ppm) as this ring aromatizes upon reaction with the adenine moiety. There are also small changes in C5 and C3α (methyl) caused by elimination of steric strain after breakage of the three-membered ring and the addition of the large adenine ring system (anisotropic effects).

Characterization of the Octamer Duplex. The oligomer used in this study is shown at the top of Figure 6 with the appropriate numbering of the nucleotides. This numbering is carried through the text and used in the tables and figures. The particular order of nucleotides in the synthesized oligomer

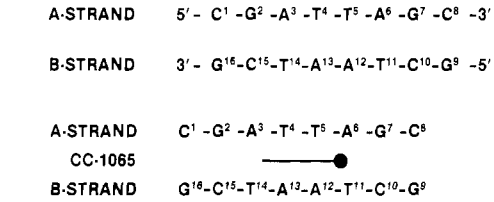

FIGURE 6: Schematic diagram of the non-self-complementary strands of the octamer duplex. The upper portions shows the numbering and sequence before addition of the drug. The lower portion shows the orientation of the drug bound to the duplex with the cyclopropyl end (A ring) designated by the large dot.

was derived from sequence-specificity results (Reynolds et al., 1985) which showed that CC-1065 has a sequence specificity. The most likely sequence for binding is the sequence 5′-Pu-N-T-T-A-3′, where Pu is any purine-containing nucleotide and N is any nucleotide. The length of the oligomer was chosen to achieve a compromise between a stable duplex with and without CC-1065 and an interpretable NMR spectrum.

The ^1H NMR of the duplex was assigned by the sequential methods previously reported (Hare et al., 1983; Scheek et al., 1984). This method uses COSY data to relate the individual spin systems within each nucleotide, i.e., H1's to H2′ and H2″ and H2′ and H2″ to H3's. NOESY data are subsequently used to identify the position of each subunit to a particular sugar and base in the sequence. The method will not be described in detail here, but a brief description of the strategy for this particular duplex will be outlined. Only a particular set of NOEs can be expected in the duplex on the basis of the distance relationships of the various forms of DNA. We expected the octamer duplex d(CGATTAGC·GCTAATCG) synthesized for this study to approximate a B-form DNA with

Table IV: Chemical Shifts[a] of the Duplex

residue	H8	H6	H5	H2	H1′	H2′	H2″	H3′	H4′
C(1)		7.53	5.80		5.74	1.87	2.38	4.61	4.24
G(2)	7.90				5.52	2.67	2.77	4.95	4.27
A(3)	8.21			7.77	6.26	2.66	2.93	4.99	4.45
T(4)		7.12	1.31		5.91	1.90	2.47	4.75	4.23
T(5)		7.30	1.57		5.65	2.04	2.37	4.61	4.06
A(6)	8.14			7.30	5.97	2.65	2.80	4.97	4.35
G(7)	7.58				5.73	2.39	2.56	4.87	4.28
C(8)		7.30	5.21		6.04	2.19	2.14	4.38	3.98
G(9)	7.90				5.91	2.66	2.77	4.87	4.20
C(10)		7.46	5.29		5.97	2.04	2.44	4.84	4.16
T(11)		7.30	1.60		5.56	2.05	2.38	4.94	4.23
A(12)	8.24			6.79	5.87	2.76	2.87	5.01	4.37
A(13)	8.10			7.53	6.09	2.45	2.84	4.90	4.40
T(14)		7.06	1.25		5.80	1.89	2.35	4.75	4.22
C(15)		7.39	5.56		5.65	1.94	2.28	4.75	4.09
G(16)	7.86				6.09	2.62	2.38	4.69	4.19

[a] In ppm relative to internal TSP.

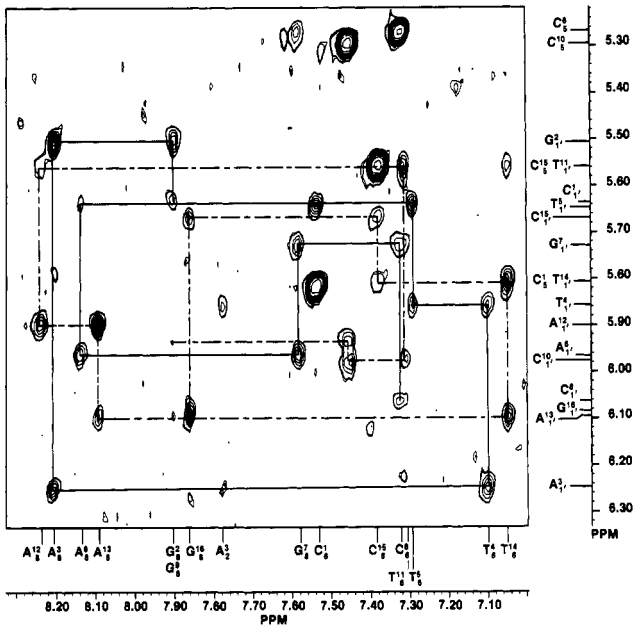

FIGURE 7: 2D NOESY contour plot of the base–H1′ region of the duplex without bound drug. The solid line traces out the sequence for the A strand (CGATTAGC) and the dashed line for the B strand (GCTAATCG).

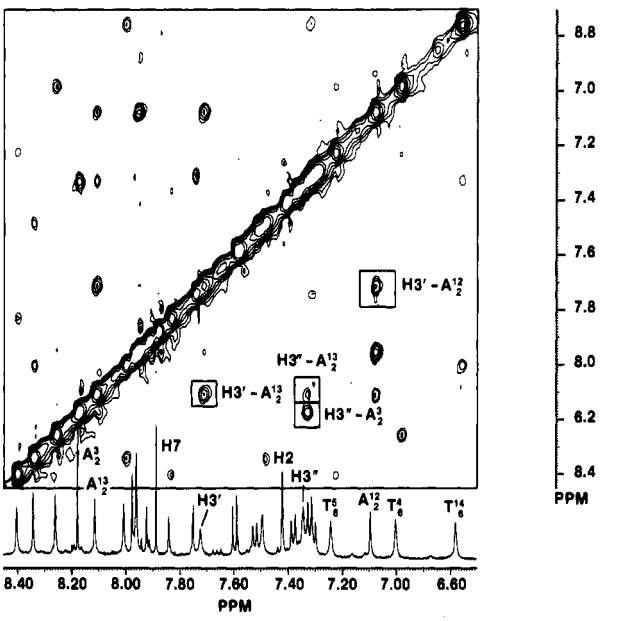

FIGURE 8: NOESY contour plot of the base–base region of the complex between CC-1065 and the octamer duplex. The boxed contours show NOE interactions between the drug protons and the adenine H2's in the minor groove of the duplex. The drug assignments are preceded by an H, and the duplex assignments are preceded with the letter A or T.

its preponderance of A's and T's in the central part of the oligomer. For example, a dipolar coupling (NOE) is expected between a purine H8 or a pyrimidine H6 and the H1′, H2′, and H2″ protons of both its own sugar and the neighboring sugar to the 5′ ($n-1$) side of the oligomer. In addition, NOEs are observed from a cytidine H5 or thymine CH3 to either a H8 or H6 of the base on the 5′ side. This is borne out in our experiments. This directional information when combined with the data from the 2D COSY experiment and the known nucleotide sequence allows the absolute assignments to be made. These assignments are listed in Table IV.

In the octamer duplex the four thymine methyls provide a convenient starting point for making the proton assignments because they are readily identifiable and do not overlap. The identification of the T(5)-CH3 is obvious because it is the only thymine methyl that has an NOE to two thymine H6 protons [T(5)-H6 and T(4)-H6]. Analysis of the COSY spectrum identifies the scalar-coupled T(5)-H6 proton, and from these data the T(4)-H6 and T(4)-CH3 can be assigned. Knowledge of these two base protons allows one to proceed with the sequential assignments by analysis of the 2D NOESY experiment in the region that correlates the base protons with the H1′ protons of the sugar residues. An expansion of this region for the 8-mer is shown in Figure 7, where the sequential assignments for strand CGATTAGC are outlined in bold lines and those for strand GCTAATCG are marked in dashed lines. The assignments proceed as follows: the vertical trace at 7.10 ppm contains two NOE cross peaks due to interaction between T(4)-H6 and [T(4)-H1′, A(3)-H1′], which absorb at 5.87 and 6.25 ppm, respectively. The absorption at 6.25 has a cross peak at 8.20 ppm, the chemical shift of A(3)-H8 (horizontal line through 6.25 ppm), and therefore can only be the H1′ of A(3), whereas T(4)-H1′ is assigned to 5.87 ppm. In this manner all the connections between H1′ and base protons are made. The same method is used to assign the proton positions of the complementary strand. When this region is completed, the H2′ and H2″ protons are assigned by analyzing the COSY and NOESY regions, relating both the anomeric hydrogens and the base protons with the H2′ and H2″ sugar protons. A careful study of the NOE correlations of the H1′, H2′, and H2″ hydrogens with the H3′ protons also leads to assignments of all the H4′ and some of the H5′ and H5″ hydrogens. Long mixing times (>300 ms) are helpful for the assignment of the

Table V: ^{1}H Chemical Shifts[a] of the Duplex Imino Protons

residues	T(3)	G(1)	C(4)
C(1)-G(16)		13.05	8.15, 6.64[b]
G(2)-C(15)		12.87	8.54, 6.98
A(3)-T(14)	13.60		
T(4)-A(13)	13.70		
T(5)-A(12)	13.60		
A(6)-T(11)	13.70		
G(4)-C(10)		12.95	8.38, 6.70
C(8)-G(9)		13.05	8.15, 6.64[b]

[a] In ppm relative to internal TSP. [b] Cannot distinguish between these iminos.

H5's since spin diffusion enhances the remote connectivities. Careful study of the COSY cross peaks, the relative intensities of the NOEs observed between all the H2′ sugar protons, the intranucleotide base proton (H8/H6), and the 3′ neighboring base proton shows that throughout the duplex the *intra*nucleotide NOE was larger than the *inter*nucleotide, signifying that sugar residues are predominantely in a 2′-endo conformation. In addition, the patterns of the COSY cross peaks (from the double-quantum filtered phase-sensitive experiment) demonstrate that the H1′–H2′ J coupling is large (9 Hz), and thus, the duplex resembles a B-form DNA structure. The duplex was also characterized in H_2O, and the imino protons were assigned by NOE difference experiments. The assignment method was the same as Chou et al. (1984), where successive imino protons are affected by irradiation of nearest neighbors. The ^{1}H chemical shifts of the imino protons are listed in Table V. Irradiation of the imino protons also afforded assignment of the minor groove adenine H2 protons. These assignments were cross-checked by observing an NOE between an adenine H2 and a H1′ of the 3′-bound nucleotide.

Characterization of the CC-1065–Octamer Complex. The assignment of the CC-1065 drug–oligomer complex was accomplished in a similar fashion to that described above. The T(4)-CH3 was assigned by identifying the methyl resonance with two NOEs to H6 protons. The T(4)-H6 proton could be distinguished from the T(5)-H6 by relating both the NOESY and COSY spectra. By use of the T(4)–H6 base proton as a convenient starting point, every H1′ and base proton on the A chain was assigned by identifying the NOEs of interresidue nucleotides through H1′(n) and base protons (n, n+1). The B strand was assigned by distinguishing between the T(11) and T(14) methyls. Analysis of the contour plots showed that one H6 proton has an NOE to A(13)-H8, A(13)-H1′, and C(15)-H6. This could be readily identified as the T(14)-H6 resonance. All the ^{1}H chemical shifts for the drug–oligomer complex are listed in Table VI, although severe overlap in the 4′, 5′, and 5″ region precluded all of these assignments. Table VII shows the differences in the chemical shifts between the oligomer duplex and the drug–oligomer complex. The data reveal some very interesting effects. For instance, relatively large shifts are observed for all of the adenine H2 resonances, signifying a large change in the minor groove environment. There are large shifts in the sugar H1′ protons of those residues that are in close proximity to the drug. There are minor shifts of the H8 protons on the bases A(6) and G(7) where the CC-1065 is covalently attached in addition to minor changes in the H6 protons of both T(11) and T(14). A careful study of the NOE spectrum shows some very important NOEs between the drug and DNA duplex, with the key groups being the CH3 (3α), H3′, and H3″ of CC-1065, the methylene groups at and adjacent to the covalent linkage between DNA and the drug, and those on the B and C rings. Specifically, strong NOEs are observed between the CH3 (3α) of the drug and A(6)-H1′, T(11)-H1′, and A(12)-H1′, and a weak NOE is seen to A(12)-H2. An NOE is observed between H2 of CC-1065 and A(12)-H1′. Proceeding along the drug molecule (i.e., in the 3′ → 5′ direction of strand A), strong NOEs are observed between CC-1065 (H3′) and A(12)-H2 and A(13)-H2 with a medium NOE to A(13)-H1′. On the C ring of CC-1065, H3″ shows a strong NOE to A(3)-H2 and a weak one to A(13)-H2. Many other minor groove NOEs are observed including CC-1065 (H4a, H5A, H5B) to A(12)-H2 and to A(6)-H2. The *more intense* NOEs observed between the head of the drug [cyclopropyl region, 3α-methyl, H2, CH_2(4), CH_2(5), CH(4a)] and A(6) (H2 and H1′) show that the drug is bound to the N3 of A(6) on strand A. The chemical shift changes of all the adenine H2's in the oligomer duplex plus the observed NOEs between these protons and CC-1065 show conclusively that the drug lies in the minor groove of the oligomer. The downfield shift of the 3α-methyl of CC-1065, the disappearance of the cyclopropyl absorptions, and the appearance of the downfield absorptions corresponding to the CH_2(4), CH_2(5), and CH(4a) groups are indicative of the opening of the cyclopropyl moiety and that the drug is *covalently bound* to the oligomer. These spectral changes are similar to that observed in the formation of the CC-1065–adenine adduct. The observation of NOEs between the CC-1065 B ring (H3′) and A(12) (H2) (medium) and A(13) (H2) (strong) and between the C ring (H3″) and A(3) (H2) (strong) and A(13) (H2) (weak) clearly demonstrates the disposition of the drug in the minor groove, i.e., extending in the 3′ → 5′ direction with the A ring near A(6). Figure 9

Table VI: ^{1}H Chemical Shifts[a] of the CC-1065–Octamer Complex

residue	H8	H6	H5	H2	H1′	H2′	H2″	H3′	H4′
C(1)		7.53	5.83		5.75	1.86	2.34	4.86	4.24
G(2)	8.03				5.52	2.63	2.72	4.95	4.28
A(3)	8.30			8.23	6.48	2.79	2.86	5.10	4.37
T(4)		7.03	1.39		5.48	1.68	1.76	4.35	3.63
T(5)		7.27	1.51		5.25	1.91	1.88	4.61	
A(6)	8.40			7.96	5.67	2.94	3.02	5.00	4.38
G(7)	7.83				5.52	2.33	2.60	4.72	
C(8)		7.36	5.33		6.19	2.18	2.40	4.60	
G(9)	7.93				5.99	2.57	2.74	4.83	
C(10)		7.51	5.39		6.00	2.04	2.35	4.84	4.16
T(11)		7.52	1.70		5.39	2.36	2.56	4.94	4.23
A(12)	8.36			7.10	6.12	2.69	2.92	5.01	4.40
A(13)	8.02			8.13	6.02	2.32	2.69	4.60	
T(14)		6.81	1.19		5.39	1.73	2.18	4.46	
C(15)		7.38	5.46		6.03	1.98	2.32	4.83	
G(16)	7.85				6.20	2.67	2.40	4.74	4.34

[a] In ppm relative to internal TSP.

Table VII: Chemical Shift[a] Changes[b] between Duplex and Drug Complex

residue	H8	H6	H5	H2	H1′	H2′	H2″
C(1)		0.00	0.03		0.01	0.01	−0.04
G(2)	0.13				0.00	−0.26	−0.05
A(3)	0.11			0.46	0.22	0.13	−0.07
T(4)		−0.09	0.08		−0.43	−0.22	−0.71
T(5)		−0.03	−0.06		−0.40	−0.13	−0.49
A(6)	0.26			0.66	−0.30	0.29	0.22
G(7)	0.25				−0.21	−0.06	0.04
C(8)		0.06	0.12		0.15	−0.01	0.26
G(9)	0.03				0.09	0.03	0.05
C(10)		0.05	0.10		0.03	0.00	−0.09
T(11)		0.22	0.10		−0.17	0.31	0.18
A(12)	0.12			0.31	0.25	−0.07	0.05
A(13)	−0.08			0.60	−0.07	−0.13	−0.15
T(14)		−0.25	−0.06		−0.41	−0.16	−0.18
C(15)		−0.01	−0.10		0.38	0.09	0.04
G(16)	−0.01				0.11	0.05	0.02

[a] All chemical shifts are in ppm relative to TSP. [b] Chemical shift differences are defined as $\Delta\delta$ = δ(oligomer–adduct) − δ(oligomer).

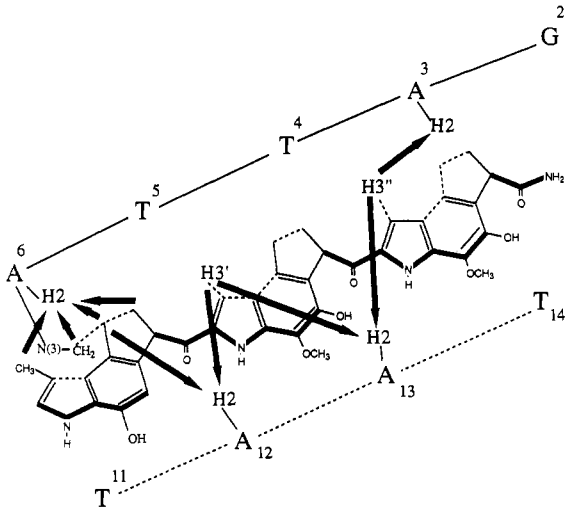

FIGURE 9: Illustration showing the disposition of the drug CC-1065 in the minor groove of the duplex along with arrows designating some observed NOEs between the drug and duplex.

shows an illustration of how the drug binds to the duplex with many of the observed NOE interactions designated by bold arrows.

Computer modeling using the X-ray coordinates of CC-1065 and standard B-form DNA shows that this arrangement results in a very compatible and snug fit on the floor of the minor groove of the oligomer. The specific NOEs and especially their relative intensities between (+)-CC-1065 and certain oligomer protons permit only *one* arrangement of the drug–oligomer complex. (+)-CC-1065 lies in the minor groove with a covalent bond between the opened cyclopropyl group (C4) and N3 of adenine-6 and extends in the 3′ → 5′ direction of strand A. Modeling the binding of the drug on any adenine of the B-strand [A(12), A(13)] will not permit a compatible fit in the groove on the basis of the *intensity differences* of the NOE data.

A limited amount of the complex prevented extensive NOE studies with various mixing times (to measure volumes and estimate distances on the basis of the NOE buildup curves), but we are currently pursuing this direction with a longer oligomer duplex. It is our hope that, with a more critical look at the distance bounds obtained from a full NOESY analysis, our NMR data will very readily complement distance geometry, energy calculations, and restrained molecular dynamics. Knowledge of this kind of detailed molecular structure will contribute not only to a better understanding of the sequence specificity of this drug but also to the design of analogues that might have different selectivity and biological activity.

ACKNOWLEDGMENTS

We gratefully acknowledge helpful discussions with C. Chidester, W. C. Krueger, and M. Warpehoski at the Upjohn Co. and with Professor Laurence Hurley at the University of Texas, Austin.

REFERENCES

Aue, W. P., Bartholdi, E., & Ernst, R. R. (1976) *J. Chem. Phys. 64*, 2229.

Bax, A., & Freeman, R. (1981) *J. Magn. Reson. 44*, 542.

Beaucage, S. L., & Caruthers, M. H. (1981) *Tetrahedron Lett. 22*, 1859.

Bodenhausen, G., Vold, R. L., & Vold, R. R. (1980) *J. Magn. Reson. 37*, 93.

Chidester, C. G., Krueger, W. C., Mizsak, S. A., Duchamp, D. J., & Martin, D. G. (1981) *J. Am. Chem. Soc. 103*, 7629.

Chou, S. H., Wemmer, D. E., Hare, D. R., & Reid, B. R. (1984) *Biochemistry 23*, 2257.

Feigon, J., Wright, J. M., Leupin, W., Denny, W. A., & Kearns, D. R. (1982) *J. Am. Chem. Soc. 104*, 5207.

Haasnott, C. A. G., Westernink, H. P., van der Marel, G. A., & van Boom, J. H. (1983) *J. Biomol. Struct. Dyn. 1*, 31.

Hanka, L. J., Dietz, A., Gerpheide, S. A., Kuentzel, S. L., & Martin, D. G. (1978) *J. Antibiot. 31*, 1211.

Hare, D. R., Wemmer, D. E., Chou, S. H., Drobny, G., & Reid, B. (1983) *J. Mol. Biol. 171*, 319.

Hurley, L. H., Reynolds, V. L., Swenson, D. H., Petzold, G. L., & Scahill, T. A. (1984) *Science 22*, 843.

Hurley, L. H., Lee, C. S., McGovern, J. P., Warpehoski, M. A., Mitchell, M., Kelly, R. C., & Aristoff, P. A. (1988) *Biochemistry 27*, 893.

Krueger, W. C., Li, L. H., Moscowitz, A., Prairie, M. D., Petzold, G., & Swenson, D. H. (1985) *Biopolymers 24*, 1549.

Krueger, W. C., Duchamp, D. J., Li, L. H., Moscowitz, A., Petzold, G. L., Prairie, M. D., & Swenson, D. H. (1986) *Chem.-Biol. Interact. 59*, 55.

Kumar, A., Ernst, R. R., & Wüthrich, K. (1980) *Biochem. Biophys. Res. Commun. 95*, 1.

Li, L. H., Wallace, T. L., DeKoning, T. F., Warpehoski, M. A., Kelly, R. C., Praire, M. D., & Krueger, W. C. (1987) *Invest. New Drugs 5*, 329.

Macura, C., Huang, Y., Suter, D., & Ernst, R. R. (1981) *J. Magn. Reson. 43*, 259.

Martin, D. G., Chidester, C. G., Duchamp, D. J., & Mizsak, S. A. (1980) *J. Antibiot. 33*, 902.

Martin, D. G., Biles, C., Gerpheide, S. A., Hanka, L. J., Krueger, W. C., McGovern, J. P., Mizsak, S. A., Neil, G. L., Stewart, J. C., & Visser, J. (1981) *J. Antibiot. 34*, 1119.

Martin, D. G., Mizsak, S. A., & Krueger, W. C. (1985) *J. Antibiot. 38*, 746.

McGovern, J. P., Clarke, G. L., Pratt, E. A., & Dekoning, T. F. (1984) *J. Antibiot. 37*, 63.

Needham-Vandevanter, D. H., Hurley, L. H., Reynolds, V. L., Theriault, N. Y., Krueger, W. C., & Wierenga, W. (1984) *Nucleic Acids Res. 22*, 6159.

Pearson, J. D., & Regnier, F. E. (1983) *J. Chromatogr. 255*, 137.

Plateau, P., & Gueron, M. (1982) *J. Am. Chem. Soc. 104*, 7310.

Redfield, A., & Kuntz, S. D. (1975) *J. Magn. Reson. 19*, 250.

Reynolds, V. L., McGovern, J. P., & Hurley, L. H. (1986) *J. Antibiot. 39*, 319.

Scahill, T. A., Brahme, N. D., Krueger, W. C., Theriault, N. Y., & Wierenga, W. (1986) *Proceedings of the 77th American Association for Cancer Research*, Los Angeles, CA, Abstract 995, Waverly Press, Baltimore, MD.

Scheek, R. M., Boelens, R., Russo, N., van Boom, J. H., & Kaptein, R. (1984) *Biochemistry 23*, 1371.

Swenson, D. H., Li, L. H., Hurley, L. H., Rokem, J. S., Petzold, G. L., Dayton, B. D., Wallace, T. L., Lin, A. H., & Krueger, W. C. (1982) *Cancer Res. 42*, 2821.

Warpehoski, M. A. (1986) *Tetrahedron Lett. 27*, 4103.